

Free Vibration Analysis of Steel-Concrete Pervious Beams

Prashant Kumar

Department of Civil Engineering, National Institute of Technology Patna, India
pk0895300@gmail.com (corresponding author)

Ajay Kumar

Department of Civil Engineering, National Institute of Technology Delhi, India
sajaydce@gmail.com

Received: 4 April 2023 | Revised: 22 April 2023 | Accepted: 24 April 2023

Licensed under a CC-BY 4.0 license | Copyright (c) by the authors | DOI: <https://doi.org/10.48084/etasr.5913>

ABSTRACT

This study investigated the free vibration analysis of steel-concrete porous beams with partial or complete shear interface using a finite-element model based on the cubic order beam theory. The present model assumes uniform porosity distribution along the beam thickness. It is assumed that the axial displacement will vary cubically along the thickness of the layer. The cubic order beam theory is implemented using a continuous C^0 finite element containing three nodes and each node has eight degrees of freedom. Shear locking is eliminated in the present model by the numerical integration of the stiffness matrix. Comparing the present model with the published literature, it is found that the present model is robust in predicting the free vibration of the steel-concrete porous beam.

Keywords-steel-concrete porous beams; finite element method; free vibration; porosity; partial shear interface

I. INTRODUCTION

New construction materials are constantly developed for various innovative engineering structures which must withstand static and dynamic loads. More and more companies are adopting cost-effective materials, while enhancing the safety and efficiency of engineering projects. Many engineering practices use composite beams, such as steel-concrete beams, in buildings and bridges, wood-concrete floors, linked shear walls, etc. [1, 2]. In structural design, it is necessary to focus on the materials and the strength of the connectors. The structure of composite beams is affected by the interlayer slip under loading. The impact of partial contact on the structural behavior was investigated in [3]. The Euler-Bernoulli beam theory was used in [4] to investigate the free vibration characteristics of steel-concrete composite continuous beams. Various experimental and analytical studies have been conducted to analyze composite beams [5]. Applying the eigenfunction expansion method along with the quasistatic decomposition method, an analytical solution is presented in [6]. Authors in [7, 8] worked on the vibrational behavior of nanocomposite beams. Under the effect of a moving load, the beam is reinforced by random straight Single-Walled Carbon NanoTubes (SWCNTs).

The accurate results of Higher-order Beam Theory (HBT) intrigued researchers, so TBT has been replaced with HBT in order to obtain more accurate solutions. Authors in [9] built on Reddy's approach to an HSST for multi-layered anisotropic

composite laminates having complete shear interaction. C^0 finite element models were presented for evaluating composite and sandwich beams and the penalty function approach was used to find a C^0 continuous finite element formulation [10, 11]. Analysis of 3 different porosity variations in the thickness direction and their impact on the vibrational properties of the beam are presented in [12]. Free and forced lateral vibration analysis of beams made from Functionally Graded Materials (FGMs) using the Finite Element Method (FEM) is presented in [13]. The state-space technique was used in [14] to expand the static analysis to dynamic analysis without the use of axial force.

From the literature review, it can be seen that there are a few studies regarding the free and forced vibration of a porous steel-concrete beam with a partial shear interface. Therefore, the present study uses the cubic order equation for axial displacement. A linear finite element model is developed for the dynamic analysis of a porous composite beam. The proposed composite beam has a partial or complete shear interaction. The homogeneous porosity distribution along the beam thickness is used to parametrically calculate the material properties. Different interfacial stiffness values are used to calculate the fundamental frequency. The present model is effective for analyzing the free vibrations of porous beams made of steel and concrete under various boundary conditions and moving loads. Several new findings are presented in this paper, making it useful for the subsequent analysis of the free vibration of porous composite beams in the future.

II. FORMULATION

A. Porosity Distribution

This study evaluates how steel and concrete porosity influence the free vibration of composite beams. Due to the uniform distribution of porosity, the variation in Young's modulus, shear modulus, and mass density of the concrete and the steel layer is calculated by:

$$\begin{cases} E_i(y) = E_{\max}(1 - \kappa_i) \\ G_i(y) = G_{\max}(1 - \kappa_i) \\ \rho_i(y) = \rho_{\max}\sqrt{1 - e_{mi}\kappa_i} \end{cases} \quad (1)$$

where $E_i(y)$, $G_i(y)$, $\rho_i(y)$ are the Young's modulus, shear modulus, and mass density of the concrete (upper) layer and steel (lower) layer of the beam along the transverse direction (where $i = c$ -concrete, s -steel).

$$e_i = 1 - \frac{E_{\min}}{E_{\max}} = 1 - \frac{G_{\min}}{G_{\max}} \quad (2)$$

$$e_{mi} = 1 - \sqrt{1 - e_i} \quad (3)$$

where the range of the porosity coefficient for mass density (e_m), porosity coefficient of concrete (e_c), and porosity coefficient of steel (e_s) are $0 < e_{mi} < 1$, and $0 < e_i < 1$. $e_i = e_{mi} = 0$ means that porosity is zero at maximum elastic modulus and greater porosity gives lower elastic modulus.

$$\kappa_i = 1 - \left(\frac{2}{\pi} \sqrt{1 - e_i} - \frac{2}{\pi} + 1 \right)^2 \quad (4)$$

B. Mathematical Formulation

High-order beam theory is used to investigate the free vibration analysis of a composite beam having a shear interface as shown in Figure 1. The displacement field that was selected is unique. Transverse shear stresses must cease on the beam surfaces and remain nonzero elsewhere for the requirements to be satisfied, which determines the shape. The beam's axial displacement is considered as the thickness's cubic function. The axial displacement equation for the upper layer is expressed in (5).

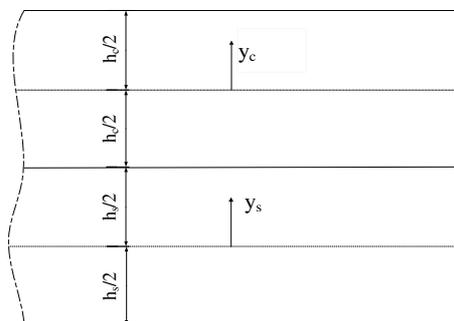


Fig. 1. Porous steel-concrete composite beam with shear flexible interface.

$$[u_i] = \begin{bmatrix} 1 & -y_i & y_i^2 & y_i^3 \end{bmatrix} [u_{i0} \quad \theta_i \quad \zeta_i \quad \xi_i]^T \quad (5)$$

where $[u_i] = u(x, y_i, z)$ is the axial displacement along the top layer's reference axis passing through its centroid, $\theta_i = \theta(x)$ is the bending rotation, and $\zeta_i = \zeta(x)$ and $\xi_i = \xi(x)$ are high-order terms.

The transverse displacement is assumed to be the same for both layers and can be represented as:

$$W_c(x, y_c, z) = W_s(x, y_s, z) = W(x) = W \quad (6)$$

The partial shear interaction between two layers of the composite beam is modelled by taking distributed shear springs at their interface. The interfacial stiffness and the shear slip at the interface are used to figure out the shear stress at the interface. Interfacial slip (s) is calculated in (7) with u'_c and u'_s being the axial displacement of the upper and lower layer at the interface.

$$s = (u'_c - u'_s) \quad (7)$$

Axial displacement equations, such as (5), are higher-order equations that are concerned with the warping of transverse sections, but do not describe the commonly used displacement parameters adopted in beam theories. So, higher order terms are eliminated by using shear stress-free conditions at the extreme surfaces of the composite beam. The shear stress at any point in the upper layer is calculated by:

$$\begin{aligned} [\tau_c] &= [G_c][\gamma_c] \\ \gamma_c &= \left\{ \frac{\partial u_c}{\partial y_c} + \frac{\partial W}{\partial x} \right\} = \begin{bmatrix} -1 & 2y_c & 3y_c^2 & 1 \end{bmatrix} \\ &\quad \times \begin{bmatrix} \theta_c & \zeta_c & \xi_c & \frac{\partial W}{\partial x} \end{bmatrix}^T \end{aligned} \quad (8)$$

where γ_c is the shear strain and G_c the shear modulus of porous concrete layer.

$$\begin{aligned} A_c &= \left\{ 1 - \left(\frac{12y^2}{5h_c^2} \right) + \left(\frac{16y^3}{5h_c^3} \right) \right\}, \\ B_c &= \left\{ \left(\frac{12y^2}{5h_c^2} \right) - \left(\frac{16y^3}{5h_c^3} \right) \right\}, \\ C_c &= \left\{ -y - \left(\frac{4y^2}{5h_c} \right) + \left(\frac{12y^3}{5h_c^2} \right) \right\}, \\ D_c &= - \left\{ \left(\frac{2y^2}{5h_c} \right) + \left(\frac{4y^3}{5h_c^2} \right) \right\} \\ A_s &= \left\{ 1 - \left(\frac{12y^2}{5h_s^2} \right) - \left(\frac{16y^3}{5h_s^3} \right) \right\}, \\ B_s &= \left\{ \left(\frac{12y^2}{5h_s^2} \right) + \left(\frac{16y^3}{5h_s^3} \right) \right\}, \\ C_s &= \left\{ -y + \left(\frac{4y^2}{5h_s} \right) + \left(\frac{12y^3}{5h_s^2} \right) \right\}, \\ D_s &= \left\{ \left(\frac{2y^2}{5h_s} \right) - \left(\frac{4y^3}{5h_s^2} \right) \right\}, \text{ and } \chi = \frac{dW}{dx} \end{aligned} \quad (9)$$

Shear stress-free conditions are applied at the top and bottom surface of the beam to find the displacement equation.

$$[u_i] = [A_i \ B_i \ c_i \ D_i] [u_{i0} \ u'_i \ \theta_i \ \chi]^T \quad (10)$$

The normal stress and normal strain at any point of the beam are calculated by:

$$\{\bar{\sigma}\}_j = [\bar{D}]_j \{\bar{\epsilon}\}_j \quad (11)$$

$$\{\bar{\epsilon}\}_j = \left\{ \begin{matrix} \epsilon_j \\ \gamma_j \end{matrix} \right\} = \left\{ \begin{matrix} \frac{\partial u_j}{\partial x} \\ \frac{\partial u_j}{\partial y_j} + \frac{\partial W}{\partial x} \end{matrix} \right\} = [H]_j \{\epsilon\}_j \quad (12)$$

where σ_j is the normal stress, τ_j the shear stress, E_j the modulus of elasticity, G_j the shear modulus, ϵ_j the normal strain, and γ_j the shear strain of the j^{th} layer, $j=c$ represents the upper layer and $j= s$ represents the lower layer of two-material composite beams. $[H]_j$ is a function of y_j and $\{\epsilon\}_j$ is the function of x_j which is coordinated along the axial direction. The expressions of $[H]_j$ and $\{\epsilon\}_j$ are:

$$[H]_j = \begin{bmatrix} A_j & B_j & C_j & D_j & 0 & 0 & 0 & 0 \\ 0 & 0 & 0 & 0 & \frac{dA_j}{dy_j} & \frac{dB_j}{dy_j} & \frac{dC_j}{dy_j} & \frac{dD_j}{dy_j} \\ & & & & & & & 1 \end{bmatrix} \quad (13)$$

$$\{\epsilon\}_j^T = \left[\frac{du_j}{dx} \ \frac{du'_j}{dx} \ \frac{d\theta_j}{dx} \ \frac{d\phi}{dx} \ u_{j0} \ u'_j \ \theta_j \ \phi \ \frac{\partial W}{\partial x} \right] \quad (14)$$

The strain energy as a function of stress and strain can be found by (11)-(12).

$$U = \frac{1}{2} \int \left(\{\bar{\epsilon}\}_c^T \{\bar{\sigma}\}_c + \{\bar{\epsilon}\}_s^T \{\bar{\sigma}\}_s \right) dA dx \quad (15)$$

$$= \frac{1}{2} \int \left(\{\bar{\epsilon}\}_c^T [D]_c \{\epsilon\}_c + \{\bar{\epsilon}\}_s^T [D]_s \{\epsilon\}_s \right) dx$$

where $[D]_c = \int ([H]_c [\bar{D}]_c [H]_c) dA_c$, $[D]_s = \int ([H]_s [\bar{D}]_s [H]_s) dA_s$

Numerical integration is used to evaluate the cross-section rigidity matrix $[D]_c$ and $[D]_s$. Stored strain energy is calculated by (7) and distributed shear springs stiffness (k_s):

$$U' = \frac{1}{2} \int k_s s^2 dx = \frac{1}{2} \int k_s (u_c - u_s)^2 dx \quad (16)$$

C. Finite Element Formulation

First of all, the 3-nodded iso-parametric C^0 element is selected. This theory assumes 8 nodal degrees of freedom to solve the present problem using a one-dimensional finite element approximation written as:

$$\{f\} = \{u_{c0j} \ u'_{cj} \ \theta_{cj} \ \chi_j \ W_j \ u_{s0j} \ u'_s \ \theta_s\}^T \quad (17)$$

The unknown nodal displacement vector $\{d\}$ on the middle surface of a typical element is given by:

$$\{d\} = \sum_{i=1}^3 \psi_i(x, y) \cdot \{d_i\} \quad (18)$$

where ψ_i is the shape function.

The generalized strain vector as a function of the nodal displacement vector $\{d\}$ can be found by:

$$\{\epsilon\}_j = \sum_{i=1}^3 [P_i] \{d_i\} \quad (19)$$

where $[P_i]$ is the interpolation function differential operator matrix.

The strain vectors are calculated by (13), (16), and (18) as a function of the stiffness matrix $[K^l]$.

$$U = \frac{1}{2} \{d\}^T [K^l] \{d\} \quad (20)$$

where:

$$[K^l] = \int \left([P]_c^T [D]_c [P]_c + [P]_s^T [D]_s [P]_s \right) dx \quad (21)$$

Similarly, the interfacial stiffness and stiffness due to the penalty function approach are given below:

$$[K^i] = \int \left([P^i]^T k_s [P^i] \right) dx \quad (22)$$

$$[K^p] = \int \left([P^p]^T k_p [P^p] \right) dx \quad (23)$$

Now we can integrate (21), (22), and (23) and combine them to find out the element stiffness matrix $[K]$.

$$[K] = [K^l] + [K^i] + [K^p] \quad (24)$$

An element's mass matrix and its geometric stiffness matrix can be found in the same way as the element stiffness matrix is calculated above. Equations (16)-(18) are used to find out the displacement component vector at a point in the beam layer:

$$\{f\} = \begin{Bmatrix} u_j \\ W \end{Bmatrix} = [F_j] \{f\} = [F_j] [X] \{d\} \quad (25)$$

where $[F_j]$ is a matrix of order 2×8 which contains the coefficient of displacement component expressed in (25) and $[X]$ is a shape function matrix of order 8×24 .

Now, the consistent mass matrix of 3-nodded elements is developed by using (25) and is expressed as:

$$[M] = \iiint [X]^T \left([F_j]^T \rho_j [F_j] dz \right) [X] dx dy \quad (26)$$

Free vibration analysis is conducted to find out the fundamental natural frequency from the given equation:

$$[K_s - \omega^2 \{M_g\}] \{\lambda\} = 0 \quad (27)$$

where ω is the vibration frequency and $\{\lambda\}$ the eigenvector.

III. RESULTS AND DISCUSSION

A finite element technique based on the cubic order beam theory was used to examine steel-concrete beam features to assess the effectiveness of the recommended model. The findings are produced by implementing the proposed model in FORTRAN code.

A. Comparison Study

For the validation of the results, a two-layered simple support composite beam having a T-cross section is considered. The four different Boundary Conditions (BCs) SS, SC, CC, and CF (SS = Simply Supported, C = Clamped, F = Free) and the partial interaction of the composite beams were taken into consideration. The results used for validation are taken [14], in which the state-step approach is used to tackle this issue. In this example, the cross-sectional size and material characteristics of a two-layered composite beam are stated as: span length (L) of beam equal to 4m, the upper and lower elements are 0.05x0.30m² and 0.15x0.05m², respectively, the modulus of elasticity of the upper (E₁) and lower elements (E₂) are 12Gpa and 8Gpa, respectively, the modulus of rigidity of the upper (G₁) and lower element (G₂) are 5GPa and 3GPa, respectively, and the mass densities of the upper and lower elements are taken as ρ₁ = 2400Kg/m³ and ρ₂ = 500Kg/m³, respectively, using partial interfacial spring stiffness k_s = 50MPa.

The free vibration frequencies (rad/s) for various BCs are listed in Table I. Fifty elements throughout the length of the beam are used to determine the present findings. The natural frequency of a Simply Supported (SS) beam determined in [14] and using the state-space technique is contrasted with the present results. The error percentages are also listed in parentheses. In the present simulation, the results are quite accurate and in close agreement with those in [14] with an accuracy of 99.76%.

TABLE I. VALIDATION OF THE FUNDAMENTAL FREQUENCY OF A COMPOSITE BEAM (E₀=E₁=0).

S.No.	BC	Fundamental frequency (rad/s)	
		Present	[14]
1.	CF	25.06	25.12 (0.24)
2.	SS	64.56	64.85 (0.45)
3.	SC	88.78	89.56 (0.88)
4.	CC	116.66	118.50 (1.58)

Note: Parameters in parentheses represent percentage errors.

B. Steel-Concrete Porous Beam

In the present study, steel-concrete two-material composite beams with different porosity, BCs, and different interfacial shear stiffness values are taken for analysis. The beam's cross-section (Figure 2) is made up of a rectangular slab with a thickness and width of 0.15m and 2.25m respectively, an I-shaped steel joist with a flange dimension of 0.1780x0.13m, and a web dimension of 0.380x0.078m. The material properties of the two layers are as follows: beam span L = 15m, the modulus of elasticity E_C and the modulus of rigidity G_C of the upper (concrete) element are 13.55GPa and 6.775GPa, respectively, and the modulus of elasticity E_S and the modulus of rigidity G_S of the lower (steel joist) element are 200GPa and 100GPa, respectively. The maximum densities of the concrete

element and the steel layer are taken as ρ_C = 2396.45Kg/m³ and ρ_S = 7948.89Kg/m³, respectively, and the uniform porosity distribution of the concrete and steel element is taken as 0, 0.05, 0.10, 0.20, 0.30, and 0.4. In the case of partial interaction, it is assumed that the interfacial shear spring stiffness k_s is 100MPa. A moving point load of magnitude 100KN is applied. The point load is traveling from the left support to the right support at a constant speed v₀ of 16.67m/s.

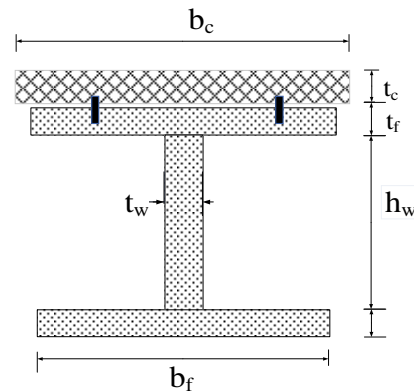


Fig. 2. Cross section of the steel-concrete porous flanged composite beam.

C. Effect of Boundary Conditions, Porosity, and Interlayer Spring Stiffness on Fundamental Frequency

In both cases, the fundamental frequency of a SS steel-concrete porous beam with partial or complete shear interface varies with the porosity as shown in Figure 3.

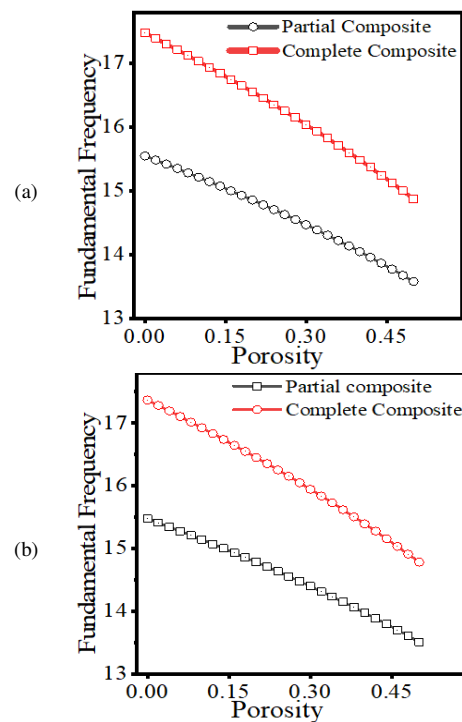


Fig. 3. Variations of fundamental frequency as a function of (a) porosity of the steel element and (b) porosity of concrete and steel elements.

It decreases with an increase in the porosity of the concrete slab and steel joist. The fundamental frequency of the steel-concrete porous beam is greater with a complete shear interface than with a partial shear interface. Table II describes the effect of the porosity of steel ($e_j=0, 0.05, 0.1, 0.2, 0.3, \text{ and } 0.4$) and BCs on the fundamental frequency of complete and partial interface steel-concrete porous beams without considering the damping effect. It is maximum for the CC (clamped, clamped) and minimum for the CF (clamped, free) BC. Table III shows

the effect of steel and concrete layer porosity variations on the fundamental frequency ($e_o=e_j=0, 0.05, 0.1, 0.2, 0.3, \text{ and } 0.4$). The different boundary conditions are considered. Table IV analyzes the impact of the interfacial shear stiffness (k_s) on the fundamental frequency. Porosity variation is taken into account in this scenario. Fundamental frequencies increase as interfacial shear stiffness increases, as can be easily seen. The fundamental frequency of a steel-concrete porous simply supported beam is expected to change with its porosity.

TABLE II. FUNDAMENTAL FREQUENCY OF POROUS BEAM FOR DIFFERENT POROSITY (e_j) AND BOUNDARY CONDITIONS

Porosity (e_j)	Fundamental frequency(rad/s)							
	Partial composite				Full composite			
	CF	SS	SC	CC	CF	SS	SC	CC
0.00	5.9217	15.5493	22.0437	29.6486	6.2464	17.4810	27.0829	38.8882
0.05	5.8527	15.3843	21.8207	29.3481	6.1676	17.2605	26.7407	38.3962
0.10	5.7815	15.2140	21.5914	29.0400	6.0863	17.0332	26.3879	37.8891
0.20	5.6318	14.8553	21.1112	28.3985	5.9155	16.5555	25.6468	36.8240
0.30	5.4703	14.4680	20.5966	27.7164	5.7320	16.0420	24.8503	35.6798
0.40	5.2944	14.0451	20.0388	26.9833	5.5327	15.4845	23.9859	34.4384

TABLE III. FUNDAMENTAL FREQUENCY OF POROUS BEAM FOR e_o, e_j , AND BOUNDARY CONDITIONS

Porosity		Fundamental frequency(rad/s)							
e_o	e_j	Partial composite			Full composite				
		CF	SS	SC	CC	CF	SS	SC	CC
0.00	0.00	5.9217	15.5493	22.0437	29.6486	6.2464	17.4810	27.0829	38.8882
0.05	0.05	5.8354	15.3453	21.7723	29.2861	6.1470	17.2027	26.6518	38.2691
0.10	0.10	5.7489	15.1407	21.5010	28.9246	6.0473	16.9239	26.2198	37.6488
0.20	0.20	5.5744	14.7276	20.9562	28.2019	5.8467	16.3625	25.3501	36.4000
0.30	0.30	5.3964	14.3058	20.4039	27.4742	5.6429	15.7920	24.4661	35.1307
0.40	0.40	5.2130	13.8700	19.8374	26.7337	5.4335	15.2062	23.5586	33.8276

TABLE IV. FUNDAMENTAL FREQUENCY OF POROUS SS COMPOSITE BEAM FOR DIFFERENT POROSITY e_o, e_j , AND INTERFACIAL STIFFNESS (k_s)

Porosity		Fundamental frequency(rad/s)							
e_o	e_j	$k_s=10^{-2}$	$k_s=10^{-1}$	$k_s=10^0$	$k_s=10$	$k_s=10^2$	$k_s=500$	$k_s=10^3$	$k_s=10^4$
		0.00	0.00	10.6498	10.6660	10.8244	12.0652	15.5493	16.9769
0.05	0.05	10.4803	10.4968	10.6577	11.9090	15.3453	16.7213	16.9527	17.1768
0.10	0.10	10.3105	10.3273	10.4909	11.7535	15.1407	16.4649	16.6858	16.8993
0.20	0.20	09.9686	09.9861	10.1557	11.4437	14.7276	15.9478	16.1479	16.3404
0.30	0.30	09.6212	09.6395	09.8164	11.1336	14.3058	15.4207	15.6003	15.7722
0.40	0.40	09.2644	09.2837	09.4695	10.8208	14.8700	14.8777	15.0371	15.1888

IV. CONCLUSIONS

In this paper, one-dimensional finite element methods based on cubic order beam theory are used to analyze the free vibration of pervious steel-concrete beams. The distribution of linear shear springs is used to simulate partial shear interaction between layers. The cubic order beam theory is implemented using a continuous C^0 finite element containing 3 nodes. This work presents a novel analysis of the effect of porosity on the fundamental frequency of layered composite beams. The main findings of this study are:

- As the porosity of the steel-concrete composite beam increases from 0 to 0.40, the fundamental frequency decreases by 10% in partial interaction and approximately 13.0% in the complete composite.
- The presented finite element formulation shows the relationship between the fundamental frequency and

various parameters such as the interfacial shear stiffness and end supports.

- In CF support, the fundamental frequency is minimum, whereas it is maximum in CC support.
- It is greater for a complete shear interface than for a partial shear interface. An increase in interfacial shear stiffness from 10^{-2} to 10^4 leads to an increase in fundamental frequency by more than 63%.
- The proposed model is more accurate in predicting the free vibration of composite steel-concrete porous beams than the existing models based on EBT and TBT.

ACKNOWLEDGMENT

The authors would like to thank the National Institute of Technology Patna (India) for its financial support.

REFERENCES

- [1] D. Mohammed and S. R. Al-Zaidee, "Deflection Reliability Analysis for Composite Steel Bridges," *Engineering, Technology & Applied Science Research*, vol. 12, no. 5, pp. 9155–9159, Oct. 2022, <https://doi.org/10.48084/etasr.5146>.
- [2] K. Swaminathan, D. T. Naveenkumar, A. M. Zenkour, and E. Carrera, "Stress, vibration and buckling analyses of FGM plates—A state-of-the-art review," *Composite Structures*, vol. 120, pp. 10–31, Feb. 2015, <https://doi.org/10.1016/j.compstruct.2014.09.070>.
- [3] A. Yasunori, H. Sumio, and T. Kajita, "Elastic-plastic analysis of composite beams with incomplete interaction by finite element method," *Computers and Structures*, vol. 14, no. 5–6, pp. 453–462, 1981, [https://doi.org/10.1016/0045-7949\(81\)90065-1](https://doi.org/10.1016/0045-7949(81)90065-1).
- [4] Q. Sun, N. Zhang, G. Yan, X. Zhu, X. Liu, and W. Li, "Exact Dynamic Characteristic Analysis of Steel-Concrete Composite Continuous Beams," *Shock and Vibration*, vol. 2021, 2021, <https://doi.org/10.1155/2021/5577276>.
- [5] H. I. Yoon, I. S. Son, and S. J. Ahn, "Free vibration analysis of Euler-Bernoulli beam with double cracks," *Journal of Mechanical Science and Technology*, vol. 21, no. 3, pp. 476–485, 2007, <https://doi.org/10.1007/BF02916309>.
- [6] Y. W. Kim, "Dynamic analysis of Timoshenko beam subjected to support motions," *Journal of Mechanical Science and Technology*, vol. 30, no. 9, pp. 4167–4176, 2016, <https://doi.org/10.1007/s12206-016-0828-8>.
- [7] M. H. Yas and M. Heshmati, "Dynamic analysis of functionally graded nanocomposite beams reinforced by randomly oriented carbon nanotube under the action of moving load," *Applied Mathematical Modelling*, vol. 36, no. 4, pp. 1371–1394, 2012, <https://doi.org/10.1016/j.apm.2011.08.037>.
- [8] Z. H. Dakhel and S. D. Mohammed, "Castellated Beams with Fiber-Reinforced Lightweight Concrete Deck Slab as a Modified Choice for Composite Steel-Concrete Beams Affected by Harmonic Load," *Engineering, Technology & Applied Science Research*, vol. 12, no. 4, pp. 8809–8816, Aug. 2022, <https://doi.org/10.48084/etasr.4987>.
- [9] J. N. Reddy, "A Simple Higher-Order Theory for Laminated Composite Plates," *Journal of Applied Mechanics*, vol. 51, no. 4, pp. 745–752, Dec. 1984, <https://doi.org/10.1115/1.3167719>.
- [10] B. S. Manjunatha and T. Kant, "New theories for symmetric/unsymmetric composite and sandwich beams with C^0 finite elements," *Composite Structures*, vol. 23, no. 1, pp. 61–73, 1993, [https://doi.org/10.1016/0263-8223\(93\)90075-2](https://doi.org/10.1016/0263-8223(93)90075-2).
- [11] K. G. Aktas and I. Esen, "State-Space Modeling and Active Vibration Control of Smart Flexible Cantilever Beam with the Use of Finite Element Method," *Engineering, Technology & Applied Science Research*, vol. 10, no. 6, pp. 6549–6556, Dec. 2020, <https://doi.org/10.48084/etasr.3949>.
- [12] M. Heshmati and F. Daneshmand, "Vibration analysis of non-uniform porous beams with functionally graded porosity distribution," in *Proceedings of the Institution of Mechanical Engineers, Part L: Journal of Materials: Design and Applications*, Aug. 2019, vol. 233, pp. 1678–1697, <https://doi.org/10.1177/1464420718780902>.
- [13] M. Azadi, "Free and forced vibration analysis of FG beam considering temperature dependency of material properties," *Journal of Mechanical Science and Technology*, vol. 25, no. 1, pp. 69–80, 2011, <https://doi.org/10.1007/s12206-010-1015-y>.
- [14] X. Shen, W. Chen, Y. Wu, and R. Xu, "Dynamic analysis of partial-interaction composite beams," *Composites Science and Technology*, vol. 71, no. 10, pp. 1286–1294, 2011, <https://doi.org/10.1016/j.compscitech.2011.04.013>.